Permafrost Active Layer Seismic Interferometry Experiment (PALSIE) and Satellite Observations

Hunter Knox[1], Robert Abbott[1], Stephanie James[1,2], Rebekah Lee[1,3], and Chris Cole[4]

[1] *Geophysics and Atmospheric Sciences, Sandia National Laboratories, Albuquerque, New Mexico, USA;* [2] *The University of Florida, Gainesville, FL, USA;* [3] *Boise State University, Boise, ID, USA;* [4] *Bureau of Land Management, Lakewood, CO, USA*

Executive Summary: We present findings from a novel field experiment conducted at Poker Flat Research Range in Fairbanks, Alaska that was designed to monitor changes in active layer thickness in real time. Results are derived primarily from seismic data streaming from seven Nanometric Trillium Posthole seismometers directly buried in the uppermost section of the permafrost. The data were evaluated using two analysis methods: Horizontal to Vertical Spectral Ratio (HVSR) and ambient noise seismic interferometry. Results from the HVSR conclusively illustrated the method's effectiveness at determining the active layer's thickness with a single station. Investigations with the multi-station method (ambient noise seismic interferometry) are continuing and have not yet conclusively determined active layer thickness changes. Further work also continues with the Bureau of Land Management (BLM) to determine if the ground based measurements can constrain satellite imagery, which provides measurements on a much larger spatial scale.

1. Motivation

The potential feedback loop that may result from climate warming of high latitudes and the associated thawing of permafrost is of great concern to current and future climate change studies and projections. As climate warms, permafrost thaws and the active layer increases in thickness (Nelson et al., 2001). In the Northern Hemisphere, frozen relict soils contained in permafrost have high carbon content (Zimov et al., 2009). Therefore, the thawing of permafrost results in decay of previously frozen organic matter which then releases carbon to the atmosphere through bacterial respiration in the form of either carbon dioxide or methane, CO_2 or CH_4, respectively (Zimov et al., 2009; Schuur et al., 2008; Schuur et al., 2009). In addition, thawing of permafrost also causes subsidence and slope destabilization, both of which are critical to infrastructure, construction operations, and produce natural hazards (Nelson et al., 2001; Gruber et al., 2007). Monitoring changes in active layer thickness from year to year (building up to decadal trends) will provide invaluable information for many entities (i.e. DOD, DOE, DHS, BLM, USGS, etc). This project was designed to evaluate the hypothesis that changes in active layer thickness exhibit a noticeable difference in seismic velocities, that those changes could be monitored in real time, and this spatially limited information could be used to calibrate satellite imagery.

2. Site Description

The site location for this study was contained within a ~0.01 km^2 area at Poker Flat Research Range (PFRR), approximately 30 miles north of Fairbanks,

Alaska. PFRR is a scientific research facility owned and operated by the Geophysical Institute of the University of Alaska. PFRR lies within the northern portion of what is known as the Fairbanks mining district of Alaska. This mining district was one of the most important gold producing areas in Alaska (Robinson et al., 1990). The site is situated along the northwest side of a slope that descends gradually to the Chatanika River, located approximately 1 km to the northwest from the site. Permafrost in the study region is discontinuous, meaning permafrost is typically no more than 50 m thick and talik zones are common (Schuur et al., 2008; Yershov, 1998). The study area is within the boreal forest ecoregion of interior Alaska as classified by Nowacki and others (2001). More specifically, PFRR lies in the Yukon-Tanana Uplands of the Intermontane Boreal ecoregion (Nowacki et al., 2001).

In the discontinuous permafrost zone that comprises our study site, permafrost generally occurs on north-facing slopes since they receive less direct radiation compared to south-facing slopes (Jorgenson et al., 2010). Also, the boreal forests of the study region can have an insulating effect on the soil, thereby contributing to factors controlling permafrost characteristics (Jorgenson et al., 2010). In turn, the presence and type of vegetation can be influenced by permafrost characteristics, and can sometimes be used as permafrost and active layer thickness/presence indicators. For example, the northwest portion of the site contains black spruce trees, which generally occur in poorly drained organic soils that are underlain by permafrost (Viereck et al., 1992). We would expect that active layer thicknesses and permafrost extents in the northwest portion are different than those in locations without black spruce trees on the study site.

3. Seismic Array

The primary data for this experiment was continuous seismic data collected with a small array deployed at PFRR. The array geometry is best described as two concentric circular arrays with 50 and 125m radii respectively. For this array, we chose to deploy seven Nanometrics Trillium Compact (TC) Posthole sensors. These state-of-the-art sensors were chosen because: 1) the instruments had self-noise levels below the USGS New Low-Noise Minimum Model (NLNM) at the frequencies of interests (> 1 Hz), 2) they are designed for direct burial, meaning they do not require a seismic vault or enclosure, and 3) the sensor has wide tilt tolerance (+/- 10 degrees from horizontal). Refraction Technologies (RefTek) Model 130 6-channel digitizers were chosen for the digital acquisition systems (DAS). The network was powered by extending 120V AC power to the center of the array from existing powered infrastructure. At the center of the array, we placed a Power-Over-Ethernet (PoE) hub, which distributed 40 Volts DC to the seven array elements. There the 40 Volts were reduced to 12 Volts by a DC-to-DC power converter. The array's close proximity to a building with power and Internet allowed us to install a physical Ethernet cable for communication. The RefTek 130s came with GPS clocks and antennas for timing. We installed the GPS antennas on T-posts high enough (about 1.5 meters) to be above the presumed snow depth.

4. HVSR Investigation

During the planning phases of this experiment, it was believed that computing the horizontal to vertical spectral ratios (HVSR) at each station would yield estimates of active layer thickness in real time. This was primarily due to the extremely high shear wave velocity contrast existing between the active layer and the permafrost. What was unknown at that time was the level of temporal resolution that could be achieved (i.e. the number of recorded days required to make a stable estimate).

We note that this method, while not obviously useful in the presence of presumably more temporally accurate methods (i.e. borehole thermometers), could supplement the existing information and provide estimates of active layer thickness for locations where it is either logistically difficult or economically unreasonable to drill a borehole, place a thaw tube, or visit the site regularly. Installing a seismic sensor in arctic conditions, as has been proven by the massive increase in the number of deployments in the last ten years, is less arduous and expensive than drilling a borehole. This method, like borehole measurements, is sensitive to only the area immediately surrounding the seismic sensor and therefore only provides spatially confined estimates. It is possible, as will be discussed later, that these measurements could be used to calibrate satellite imagery, which could provide estimates of active layer thickness and it's temporal response over much larger areas.

HVSRs are considered standard observations for shallow site classification (i.e. VS30, VS10), making it a widely applied methodology. The work using these observations spans a great number of applications from basement depth investigations to civil structure vulnerability assessments to depth determinations for remotely located shallow subsurface layers (e.g. Nakamura, 2009; Overduin et al., 2015). The computational routine used for our investigation relied on the GEOPSY software (www.geopsy.org) and used standard processing procedures as described in SESAME (2004). More information about the general technique can be found through those references. We will highlight study specific information below.

For this study, we report analysis from 3 stations installed by Sandia National Labs (SNL) in a valley with marshy summer conditions. These stations continuously recorded data at 125 samples per second. The data from 12AM to 4AM local time was selected for evaluation and a short-term average over long-term average (STA/LTA) algorithm was used to eliminate any high amplitude events. This time period was chosen because it was the least contaminated with spurious anthropogenic noise sources. During the initial evaluation of the HVSR observations, we found that stacking a week of observations provided a stable estimate (i.e. no significant deviations were seen in the spectral responses).

Results from this study, as illustrated in Figure 1, show seasonal peaks for stations CE1 and R1B, which were installed in a deforested region with relatively consistent active layer thicknesses (determined through tile probe measurements). Figure 1 also shows that station R2C, which is located in a black spruce forest, has no obvious seasonal trend. Specifically, the results show that during the winter months, when the ground is frozen to the surface, the stations exhibit flat spectral ratios above 6 Hz. As the ground thaws from the surface downward, there is increased variation at higher frequencies. We also observed a persistent peak at 2.5 Hz, which likely represents the depth to basement rock.
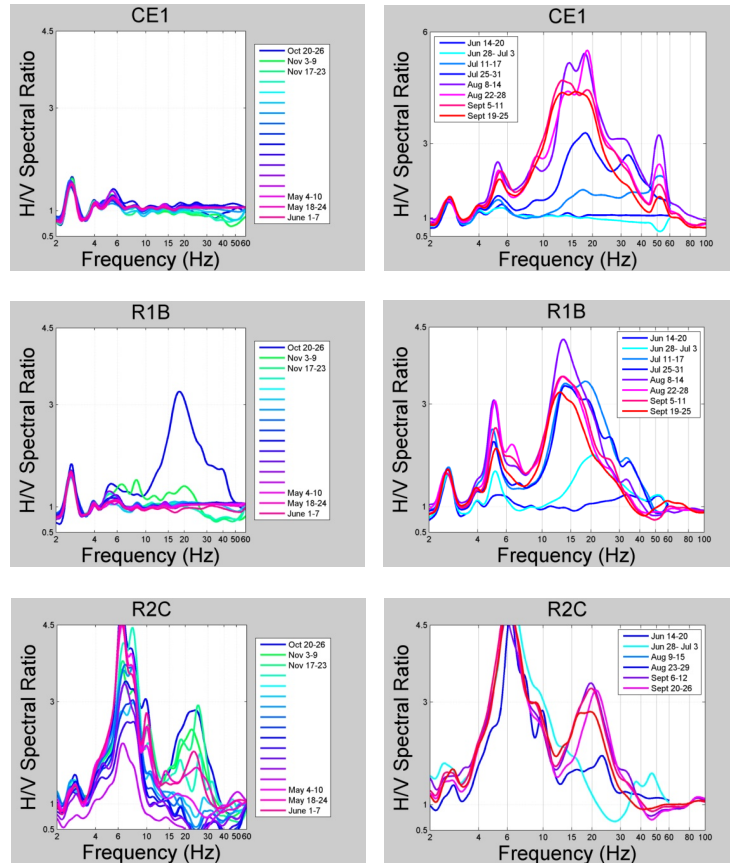

Figure 1: HVSR results for three stations at PFRR. The left column shows results for the winter months, while the right column illustrates the results for the summer months. Clear differences are seen between the stations that are likely tied to the terrain where the instruments were deployed.

We take this analysis one step further by using the quarter-wavelength approximation to estimate the active layer thickness. These thicknesses were computed for times when ground truth observations were taken. Using the quarter-wavelength approximation with h= 45 cm (thickness provided by June ground truth probing experiment), and Vs = 100 m/s (Holzer et. al, 2005; mud Vs) results in a peak at 55 Hz. This agrees nicely with the high frequency secondary peak. This peak migrates to 35 Hz, where a small shoulder is seen in HVSR, for 68 cm depth (October ground truth). These results support applicability of this method for determining

seasonal changes. The quarter-wavelength approximation however cannot be used to explain the entire spectrum (i.e. peaks at ~15 Hz for summer CE1). We believe the larger amplitude peaks are caused by changes in Rayleigh-wave ellipticity. This effect has been shown to dominate in the presence of an extremely low-velocity surface layer (Flores et al., 2014).

5. Ambient Noise Seismic Interferometry

As research into ambient seismic noise characteristics expands, so too are the number of techniques for extracting valuable subsurface information from the noise wave field. In addition to the single-station HVSR method described earlier, records of ambient noise can also be used in multi-station methods. In particular, the most common technique for processing ambient seismic noise relies on the cross-correlation of records from a pair of stations. Under the assumption of a continuous and diffuse wave field generated by numerous natural and/or anthropogenic sources, the waves that are recorded at one station and propagate towards, and are recorded by, a second station can be cross-correlated to extract the impulse response (or Green's Function, GF) of the ground between the two stations (Shaprio & Campillo, 2004; Shapiro et al., 2005). With this technique, the first station becomes a virtual source for the seismic wave; therefore information about the actual source location is not needed. This gives ambient noise an advantage over traditional seismic methods involving ballistic waves generated from specific sources such as earthquakes or explosions (Shaprio & Campillo, 2004; Shapiro et al., 2005).

Having a 2-D array of stations and cross correlating all possible station pairs samples the subsurface repeatedly and provides a group velocity dataset than can then be used for tomographic inversion. In addition, the ambient noise wavefield is largely composed of surface seismic waves, i.e. Rayleigh and Love waves, which are dispersive, meaning different frequencies have different depth sensitivities. Differences in depth sensitivity provide vertical resolution, which is necessary for obtaining vertical velocity profiles. Using this conceptual set-up, numerous studies have successfully used ambient seismic noise for regional and continental scale 2-D and 3-D tomographic inversions for crustal structure (Shapiro et al., 2005; Sabra et al., 2005; Moschetti et al., 2007; Yang et al., 2007; Lin et al., 2008). However, recent studies have also been successful in exploiting later arrivals (coda) in ambient noise cross-correlations (CCs) for tracking temporal variations in subsurface velocity (Sens-Schonfelder & Wegler, 2006; Wegler & Sens-Schonfelder, 2007; Brenguier et al., 2008; Duputel et al., 2009; Mordet et al., 2010; Brenguier et al., 2011; Mainsant et al., 2012).

We used almost two years of nearly continuous ambient noise records from the 7 station PALSIE array to construct daily cross-correlation functions. The python package MSNoise was used to pre-process and calculate the correlations. We refer the reader to Bensen et al. 2007 and Lecocq et al. 2014 for more detailed information on the cross-correlation procedure. In addition to daily CCs, the

MSNoise package allowed for moving window stacks of pre-specified numbers of days to be computed. The correlations were then used for two separate multi-station ambient noise methods. The first method consisted of measuring the travel-time of the direct wave in order to construct group velocity dispersion curves to be inverted for 1-D shear velocity profiles. The main goal of this method was to assess if seasonal changes in the vertical velocity profiles resulting from winter versus summer dispersion curves could be retrieved. Detailed resolution of changes in active layer thickness was the main target, though shifts in permafrost depth range and thickness were also of interest. The second method employed was the Moving Window Cross-Spectral (MWCS) method using the python package MSNoise in order to construct semi-continuous time series depicting perturbations in subsurface velocity. The main goal of this method was to determine if ambient noise could be used for continuous monitoring of annual changes in active layer thickness as well as long-term degradation of permafrost resulting from climate change.

a. Group-Velocity Dispersion Curves & Vertical Velocity Profiles Results

The primary objective with respect to making measurements of group velocity was to determine if the GF resulting from correlations of ambient noise was seasonally affected. Changes from frozen ground in the winter to thawed ground in the summer results in a significant decrease in rigidity, which subsequently influences the velocity at which seismic waves propagate. Studies have documented reduced seismic velocities in thawed soil compared to frozen (Barnes, 1966; Zimmerman & King, 1986; Kneisel et al., 2008). Therefore, we hypothesized that the seasonal thawing of the active layer should be observable through a decrease in seismic velocity in summer compared to winter. The vertical transition between frozen and thawed soil at the permafrost table was expected to result in a velocity drop at a specific frequency range corresponding to waves most sensitive to the active layer. Thus, by utilizing the dispersive nature of surface waves it was hoped that the specific thickness of the active layer could be obtained.

We find that: 1) at low frequencies the summer and winter CCs are very similar and produce the same group velocity, 2) at a mid-high frequency range the summer signal-to-noise ratio is lower compared to the winter and the summer group velocity is significantly slower, and 3) at high frequencies the summer arrival is even slower still and the SNR remains lower compared to winter. The winter group velocity remains static between all three-frequency bands. We note here that frequency bandwidth had a large effect on the frequency-time plots and subsequent group velocity measurements. Another complication encountered was the prominence of multiple waveforms in the CCs. Stacking longer time periods helps to stabilize the CCs and typically results in the strong emergence of the direct arrival since that path is the shortest and most common compared to random scattered paths. However, even after stacking an average of 90 winter days and 85 summer days persistent arrivals continued to stack positively resulting in multiple prominent waveforms.

The network average winter and summer dispersion curves show similar velocities at frequencies below ~35 Hz (Figure 2). At higher frequencies a clear separation between the dispersion curves is observed, where the winter dispersion curve has consistently faster group velocities compared to summer.

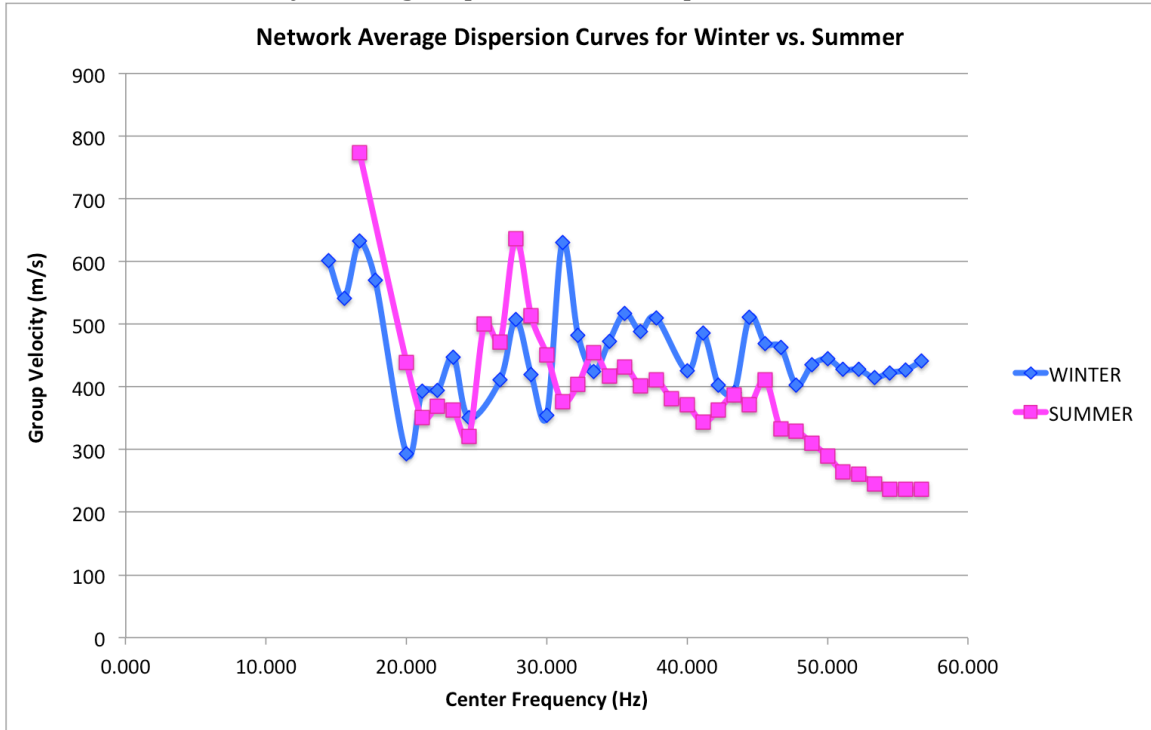**Network Average Dispersion Curves for Winter vs. Summer**

Figure 2: Network average dispersion curves for winter and summer. Note that the higher frequencies (> 35 Hz) show the most separation between winter and summer and are also better resolved compared to lower frequencies, which show more scattered.

The inversion results of the winter and summer dispersion curves show similar velocity structure below 6 meters depth (Figure 3). Above 6 m depth the winter velocity profile shows constant fast velocities within the range normal for frozen silt and organic rich soil (Barnes, 1966). The summer velocity profile shows slow velocities that gradual increase to 6 m depth. The depth sensitivity kernels produced by CPS show that the upper frequencies of the dataset have high sensitivity above ~5-6 m depth, however the sensitivities are the same in that depth range. This indicates that vertical resolution of the dataset is not sufficient to detect the specific thickness of the active layer. However, the slower velocities of the summer dispersion curve still produce a slow velocity zone at the shallowest depths. The maximum depth sensitivity of the dataset diminishes below ~24 meters depth.
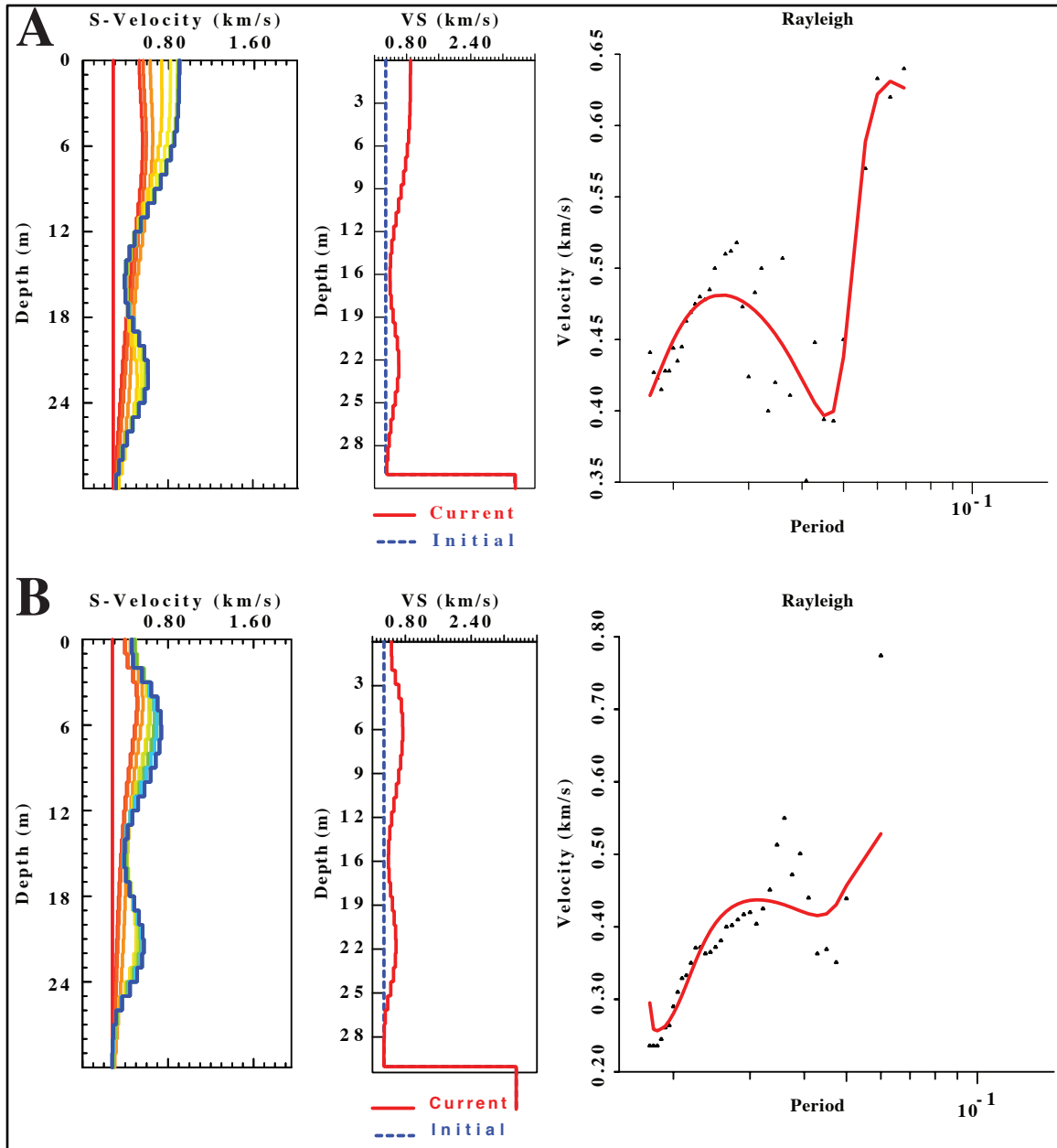
Figure 3: Results from iterative inversion using Computer Programs in Seismology (Herrmann & Ammon, 2002). Both winter (A) and summer (B) inversions start with the same constant velocity initial model (red in leftmost plots, blue in center plots). In subfigure (A), the final shear velocity profile (blue line in leftmost plot) resulting from the network average winter dispersion (center and rightmost plots) shows fast velocities from the surface down to 6 m depth followed by a gradual decrease to 15 m and subsequent increase to 22 m depth. In subfigure (B), the final shear velocity profile (blue line in leftmost plot) resulting from the network average summer dispersion (center and rightmost plots) shows slow velocities near the surface that increase down to 6 m depth followed by a decrease and increase matching that seen in the winter model. Both models navigate back toward the starting model below 24 meters depth, which is consistent with the maximum depth sensitivity.

b. Temporal Variation Results

The use of scattered seismic waves to monitor velocity changes of the subsurface was first proposed in the 1980s through analysis of seismic coda waves (Poupinet et al., 1984). This technique was later named Coda Wave Interferometry (CWI) (Snieder et al., 2002; Snieder, 2006). However, CWI relies on repetition of active sources, e.g. earthquakes, which can thereby result in discontinuous monitoring (Sens-Schonfelder & Wegler, 2006; Hadziioannou et al., 2009). Recent studies have sought the advantages of ambient seismic noise for use in monitoring applications, through a technique named Passive image interferometry (PII). PII combines the basic procedure of ambient noise cross-correlation with CWI to return measurements of temporal variations in seismic velocities of multiply scattered waves (Sens-Schonfelder & Wegler, 2006; Brenguier et al., 2008; Hadziioannou et al., 2009; Sens-Schonfelder & Wegler, 2011). PII has proven effective for a variety of applications such as detection of magma movement and changes in a volcanic edifice prior to eruption (Brenguier et al., 2008; Duputel et al., 2009; Mordet et al., 2010; Brenguier et al., 2011), co-seismic changes in fault-zone stress field (Wegler & Sens-Schonfelder, 2007), landslide prediction (Mainsant et al., 2012), and seasonal variations in hydrologic conditions (Sens-Schonfelder & Wegler, 2006).

Relative velocity changes were calculated for all station pairs for a variety of parameters and initial results from this analysis using the procedure defined by MSNoise are promising. A general trend is observed of more stable, lower amplitude $\delta v/v$ variations in winter followed by high amplitude variability in summer, regardless of the reference stack (January versus yearly average). An interesting outcome is the lack of a clear pattern of negative $\delta v/v$ values in summer and positive $\delta v/v$ values in winter. The summer months show both faster and slower velocities compared to the reference, which in the case of a January reference, is unexpected. There are a couple possible explanations for this: 1) the system could be more dynamic and complex than the simple transition from frozen to thawed ground as assumed, 2) that cycle skipping within the MSNoise analysis produces inaccurate measurements.

Overall, the findings from this portion of the PALSIE project indicate that monitoring velocity changes using ambient seismic noise is a promising new technique for permafrost studies. However, application of this method to the unique setting and characteristics of the Poker Flat dataset have led to complications not previously encountered in the seismic literature. Therefore customized procedures need to be developed.

6. Ground Truth Measurement Discussion

Here we summarize the three traditional (i.e. more common) datasets acquired throughout the course of the project. These datasets were acquired for two purposes: 1) To compare our results with more established methods; and 2) To use the results as constraints (i.e. ground truth) for the ambient noise methods. The CS survey adequately determined bulk velocities deeper than 3 meters. Coupled with

the drilling reports, the method was also able to definitively measure the depth-to-bedrock. Unfortunately, the inability of the method to resolve shallow layers in this situation is a fatal weakness, as the active-layer was shallower than the uppermost resolved layer. Also, unknown factors (i.e. poor grout coupling, potential cross talk between the instrumentation) caused poor signal quality at certain depth intervals. ReMi measurements were extremely time consuming and difficult to acquire. Poor source and receiver coupling led to bandwidth-constrained dispersion curves. This in turn led to depth reconstructions, while consistent with tile probe measurements that poorly resolved deeper velocities and exhibited a general lack of uniqueness. Not surprisingly, as they are the "standard" method of active-layer thickness measurements, tile probing proved to be the most satisfactory method. Of course, it too suffers from the requirement of costly site visit, the resultant sparsity of the year-to-year datasets resulting, and the lack of any spatial and temporal resolution below the top of the permafrost. The latter could be important for understanding the deeper effects of changing active layer thickness in discontinuous permafrost regions.

All told, fusing the three methods yielded some improvement for determining the shallow velocity structure at the site. ReMi was unable to resolve deeper layers, while CS was unable to resolve shallower ones. ReMi suffered from non-uniqueness, but fixing active layer thickness with tile probe measurements and deeper velocity from CS resulted in an adequate model for our purposes.

7. Corresponding Satellite Observations

Permafrost changes and disturbances in Alaska pose potential human and environmental impacts, which must be tracked and characterized. Due to its geographic size, and varying climate, it is impractical to monitor all permafrost cover in Alaska using manual surveying methods. The ability to monitor permafrost cover trends using deployed, *in-situ* instruments (such as the array described here), and to integrate these measurements with multi-temporal remotely sensed imagery, would prove greatly beneficial to Alaska stakeholders (i.e. Bureau of Land Management).

Multi-scale, multi-temporal remotely sensed data were used for this study. Specifically, passive electro-optical (EO) imagery systems – those that require illumination from an external power source (i.e., the Sun) were used, including high-resolution commercial WorldView-2 and WorldView-3, and synoptic Landsat missions 5 and 8. A small number of WorldView-2 and WorldView-3 scenes were also available for this study. Additionally, landsat offered a multi-decadal historical archive, which was leveraged for this study. Lastly, multiple Synthetic Aperture Radar (SAR) systems were used, because of their ability to collect information regardless of solar illumination or weather condition. These SAR instruments chiefly included commercial Radarsat-2, and the European Space Agency's new Sentinel-1A instrument.

Image processing was needed for all but the Landsat data to allow quantitative geospatial analysis. This chiefly involved orthocorrection using digital elevation model (DEM) information to reduce geometric distortions, and increase geospatial positional accuracy. Additionally, all SAR data were calibrated to sigma-naught (Radar Cross Section) to allow quantitative pixel comparisons between sensor image dates. Finally, individual SAR scenes were "stacked" to form multi-band, time series image composites, based upon the sensor type (i.e., Radarsat-2, Sentinel-1A) and type of pass (ascending, descending). This was done to allow the images to be qualitatively assessed using traditional image interpretation techniques, and to allow image-to-image change detection. Finally, this also facilitated efficient extraction of pixel values for statistical trend analysis.

An object-oriented approach was used to develop a dataset, which could be used to identify spatio-temporal trends at PFRR. Using this approach, raster data pixels are grouped into meaningful image objects (vector polygons), based upon their spatial and spectral characteristics. An image segmentation (vector) dataset was produced from the high-resolution WorldView-3 imagery spanning the study area. Pixel value statistics were calculated for each Radarsat-2 and Sentinel-1A scene date, for each image object (including Poker Flat). The final vector polygon dataset contains the mean, median, minimum, and maximum pixel statistics extracted from each SAR image date.

The time series stacks for Radarsat-2 and Sentinel-1A were analyzed using several techniques. First, an interpretative (qualitative) analysis was performed, to identify and understand changes in landcover, or changes in landcover state, over the greater study area of interest. A time series analysis was then performed using the image segmentation dataset (populated with imagery pixel statistics). This allowed the identification of spatio-temporal trends over time and by sensor.

The use of Google Earth Engine (GEE) was also investigated and employed for this study. GEE is a cloud computing architecture, which allows the user to efficiently access, process, analyze, and develop products from large geospatial data archives. GEE proved greatly beneficial to this project, as it facilitated the analysis of spectral trends of land and water cover at PFRR over multiple decades by leveraging the entire U.S. Geological Survey (USGS) Landsat archive. This was accomplished without having to download the satellite data archive, nor devote local computational resources to process this massive dataset. Without the use of GEE, this analysis would not have been possible given the project's resources. As such, GEE clearly provides an emergent tool for the scientific community.

We developed custom GEE scripts, which calculated multiple spectral indices (shown to be useful for land and water cover studies) from available Landsat 5 and Landsat 8 data from 1984 to the present. The spectral indices included Normalized Difference Vegetation Index (NVDI), Normalized Difference Snow Index (NDSI, and Normalized Difference Water Index (NDWI). The script then extracted the median pixel values for each of the spectral indices (derived from each Landsat scene)

spanning the study area, and produced a time series chart. This provided an unparalleled ability to characterize and visualize spatio-temporal spectral trends over the study site through multiple decades.

Preliminary results note a strong relationship between seasonal trends and remotely sensed observations. Our work suggests that spectral response in EO data, and in SAR backscatter measurements, differed with time of season. NDVI measurements at PFRR decreased strongly in winter, and increased strongly from spring to summer. This trend is likely due to phenology – that is, the increase in photosynthetic activity ("greenup") during the late spring and summer, and corresponding decrease in late fall to winter. Conversely, NDSI measurements at the site increased strongly in late fall to winter, and decreased significantly in summer. This is due to the presence of snow and/or ice cover. Time series analysis suggest SAR backscatter measurements followed a trend similar to that of the NDVI measurements - that is, an increase in backscatter during late spring to summer, followed by a decrease in winter. This trend was also confirmed by qualitative, interpretative analysis of the SAR multi-temporal imagery, and through change detection products derived from multiple SAR scene dates.

Conclusions

We presented here results from a two-year investigation that aimed to monitor active layer thickness in real time and link those observations (at least qualitatively) to satellite observations. Each part of this project yielded valuable information about the method's ability to determine active layer thickness, its spatial and temporal resolution, and the future challenges that must be overcome for these methods to be utilized. The HVSR method proved to be the most reliable and definitive in active layer thickness determinations, while the ambient noise seismic interferometry investigation showed complex results (previously undocumented) that will require future research. We also presented a way to combine ground truth data when each method is found to have weaknesses. Furthermore, we illustrated the difficulties in acquiring crosshole seismic and REMI data in these conditions. Finally, we present very preliminary results for the observations gained through analysis of satellite imagery. This work has only been conducted for a few short months, but shows great promise.

Path Forward

Future work on this project should continue on three fronts (HVSR, ambient noise seismic interferometry, and satellite observations), which we briefly highlight below. First, concerning the HVSR method and it's ability to determine active layer thickness, it will be paramount to invert the HVSR results with methodologies that can account for both Raleigh wave ellipticity and body wave resonances. The applicability of ambient noise seismic interferometery will require a more substantial amount of effort. Future work on this front includes conducting more rigorous group velocity measurements, evaluation of different stacking

methodologies, evaluate spatial variation in the dispersion curves, generate sensitivity kernels for synthetic dispersion curves of frequencies higher than 60 Hz to identify the frequency range needed for resolving the active layer thickness, and running Markov Chain Monte Carlo (MCMC) inversions on representative group velocity dispersion curves (winter, winter-summer transition, summer, summer-winter transition) as alternate inversion method to the iterative method in CPS. Future work for the satellite comparison should include the acquisition and analysis of follow on Landsat 8, Sentinel-1A SAR, and ALOS PALSAR-2 remotely sensed imagery. The latter two instruments operate at different wavelengths (C- and L-Band, respectively), and offer different abilities to penetrate and resolve terrestrial cover information. While C Band SAR such as Sentinel-1A are very sensitive to surficial changes and disturbances, L-Band instruments such as ALOS are able to penetrate ground, and could be beneficial in characterizing permafrost, particularly when considering InSAR measurements. Also, the use of GEE should be further explored for this project as well. This could facilitate the integration of other geospatial datasets, including meteorological data and multi-scale remotely sensed observations into our methodological framework. GEE has begun ingesting Sentinel-1A SAR information into its burgeoning archive; this could streamline our efforts greatly. Finally, GEE offers numerous analytical capabilities and data classification algorithms not yet fully explored at present.

References

Abbott, R.E. (2013), Seismic Spatial Autocorrelation as a Technique to Track Changes in the Permafrost Active Layer, Abstract C43A-0661 presented at 2013 Fall Meeting, AGU, San Francisco, Calif., 10-14 Dec.

Brenguier, F., Shapiro, N.M., Campillo, M., Ferrazzini, V., Duputel, Z., Coutant, O., & Nercessian, A. 2008. Towards forecasting volcanic eruptions using seismic noise. Nature Geoscience, 1. 126-130.

Brenguier, F., Clarke, D., Aoki, Y., Shapiro, N.M., Campillo, M., & Ferrazzini, V. 2011. Monitoring volcanoes using seismic noise correlations. Comptes Rendus Geoscience, 343, 633-638.

Campillo, M., & Paul, A. 2003. Long-range correlations in the diffuse seismic coda. Science, 299, 547-549.

"Chatanika River Mine, Fairbanks District, Fairbanks North Star Borough, Alaska, USA,". 8-7-15. http://www.mindat.org/loc-196874.html

Duputel, Z., Ferrazzini, V., Brenguier, F., Shapiro, N., Campillo, M., & Nercessian, A. 2009. Real time monitoring of relative velocity changes using ambient seismic noise at the Piton de la Fournaise volcano (La Reunion) from January 2006 to June 2007. Journal of Volcanology and Geothermal Research, 184, 164-173.

Flores, J.P., Garcia-Jerez, A., Luzon, F., Perton, M., F. Sanchez-Sesma. *Inversion of H/V ratio in layered systems*. AGU Fall meeting 2014.

Gruber, S., & Haeberli, W. 2007. Permafrost in steep bedrock slopes and its temperature-related destabilization following climate change. Journal of Geophysical Research, 112, F02S18.

Hadziioannou, C., Larose, E., Coutant, O., Roux, P., & Campillo, M. 2009. Stability of monitoring weak changes in multiply scattering media with ambient noise correlation: laboratory experiments. Journal of Acoustical Society of America, 125, 3688-3695.

Jorgenson, M. T., Shur, Y. L., & Pullman, E. R. (2006). Abrupt increase in permafrost degradation in Arctic Alaska. Geophysical Research Letters, 33(2).

Jorgenson, T. Yoshikawa, K., Kanevskiy, M., Shur, Y., Romanovsky, V., Marchenko S., Grosse, G., Brown, J., & Jones, B. 2008. Permafrost Characteristics of Alaska. Ninth International Conference On Permafrost (map).

Lee, R.F., R. E. Abbott, H. A. Knox, and A. Pancha (2014), Seasonal Changes in H/V Spectral Ratio at High Latitude Seismic Stations, Abstract S41A-4438 presented at 2014 Fall Meeting, AGU, San Francisco, Calif., 15-19 Dec.

Lin, F.C., Moschetti, M.P., & Ritzwoller, M.H. 2008. Surface wave tomography of the western United States from ambient seismic noise: Rayleigh and Love wave phase velocity maps. Geophysical Journal International, 173, 281-298.

Lobkis, O.I., & R.L Weaver. 2001. On the emergence of the Green's Function in the correlations of a diffuse field." Journal of Acoustical Society of America ,110. Sens-Schonfelder, C., & Wegler, U. 2006. Passive image interferometry and seasonal variations of seismic velocities at Merapi Volcano, Indonesia. Geophysical Research Letters, 33, L21302.

Louie, J. N., 2001, Faster, better: Shear-wave velocity to 100 meters depth from refraction mi-crotremor arrays: Bulletin of the Seismological Society of America, 91, no. 2, 347–364.

Mainsant, G., Larose, E., Bronnimann, C., Jongmans, D., Michoud, C., & Jaboyedoff, M. 2012. Ambient seismic noise monitoring of a clay landslide: Toward failure prediction. Journal of Geophysical Research, 117, F01030.

McMechan, G.A., and Yedlin, M.J., 1981, Analysis of dispersive waves by wavefield transfor-mation: Geophysics, v. 46, p. 869-874.

Mordret, A., Jolly, A.D., Duputel, Z., & Fournier, N. 2010. Monitoring of phreatic eruptions using interferometry on retrieved cross-correlation function from

ambient seismic noise: Results from Mt. Ruapehu, New Zealand. Journal of Volcanology and Geothermal Research, 191, 46-59.

Mortensen, J.K. 1992. Pre-Mid-Mesozoic Tectonic Evolution of the Yukon-Tanana Terrane, Yukon and Alaska. Tectonics, 11. 836-853.

Nelson, F., Brown, J., Lewkowicz, T., & Taylor, A. (1996). Active layer protocol.ITEX manual, 14-16.

Nelson, F.E., Anisimov, O.A., & Shiklomanov, N.I. 2001. Subsidence risk from thawing permafrost. Nature, 410, 889.

Newberry, R.J., Bundtzen, T.K., Clautice, K.H., Combellick, R.A., Douglas, T., Laird, G.M., Liss, S.A., Pinney, D.S., Reifenstahl, R.R., & Solie, D.N. 1996. Preliminary Geologic Map of the Fairbanks Mining District, Alaska. State of Alaska Department of Natural Resources, Division of Geological & Geophysical Surveys, Public-Data File 96-16.

Nowacki, G., Spencer, P., Brock, T., Fleming, M., & Jorgenson, T. 2001. Ecoregions of Alaska and Neighboring Territory. U.S. Geological Survey Open-File Report 02-297 (map).

Robinson, M.S., Smith, T.E., & Metz, P.A. 1990. Bedrock Geology of the Fairbanks Mining District. Alaska Division of Geological & Geophysical Surveys Professional Report 106, 2 sheets, scale 1:63,360. doi:10.14509/2287

Sabra, K.G., Gerstoft, P., Roux, P., Kuperman, W.A., & Fehler, M.C., 2005. Surface wave tomography from microseisms in Southern California. Geophysical Research Letters, 32, L14311.

Sens-Schonfelder, C., & Wegler, U. 2011. Passive image interferometry for monitoring crustal changes with ambient seismic noise. Comptes Rendus Geoscience, 343, 639-651.

Shapiro, N.M., & Campillo, M. 2004. Emergence of broadband Rayleigh waves from correlations of the ambient seismic noise. Geophysical Research Letters, 31, L07614.

Shapiro, N.M., Campillo, M., Stehly, L., & Ritzwoller, M.H. 2005. High-resolution surface-wave tomography from ambient seismic noise. Science, 307, 1615-1618.

Schuur, E.A.G., Bockheim, J., Canadell, J.G., Euskirchen, E., Field, C.B., Goryachkin, S.B., Hagemann, S., Kuhry, P., Lafleur, P.M., Lee, H., Mazhitova, G., Nelson, F.E., Rinke, A., Romanovsky, V.E., Shiklomanov, N.,Tarnocai, C., Venevsky, S., Vogel, J.G., & Zimov, S.A. 2008. Vulnerability of permafrost carbon to climate change: Implications for the global carbon cycle. Bioscience, 58, 701-714.

Schuur, E.A.G., Vogel, J.G., Crummer, K.G., Lee, H., Sickman, J.O., & Osterkamp, T.E. 2009. The effect of permafrost thaw on old carbon release and net carbon exchange from tundra. Nature, 459, 556-559.

Snieder, R. , Gret, A., Douma, H., & Scales, J. 2002. Coda Wave Interferometry for estimating nonlinear behavior in seismic velocity. Science, 295, 2253-2255.

Snieder, R. 2006. The theory of Coda Wave Interferometry. Pure and Applied Geophysics. 163. 455-473.

Viereck, L.A., Dyrness, C.T., Batten, A.R., Wenzlick, K.J. 1992. The Alaska Vegetation Classification. United States Department of Agriculture, Forest Service, General Technical Report PNW-GTR-286.

Weaver, R.L., & Lobkis, O.I. 2001. Ultrasonics without a source: Thermal fluctuation correlations at MHz frequencies. Physical Review Letters, 87, 134301.

Wilson, F.H., Dover, J.H., Bradley, D.C., Weber, F.R., Bundtzen, T.K., & Haeussler, P.J. 1998. Geologic Map of Central (Interior) Alaska. U.S. Geological Survey Open-File Report OF 98-133

Yang, Y., Ritzwoller, M.H., Levshin, A.L., & Shapiro, N.M. 2007. Ambient noise Rayleigh wave tomography across Europe. Geophysical Journal International, 168, 259-274.

Yershov, E. 1998. General Geocryology. Cambridge (United Kingdom): Cambridge University Press.

Zimmerman, R.W., & King, M.S. 1986. The effect of the extent of freezing on seismic velocities in unconsolidated permafrost. Geophysics, 51, 1285-1290.

Zimov, S.A., Schuur, E.A.G., Chapin III, F.S. 2009. Permafrost and the global carbon budget. Science, 312, 1612-1613.